ISSN: 2230-9926

Available online at http://www.journalijdr.com

IJDR

International Journal of Development Research
Vol. 11, Issue, 05, pp. 47270-47275, May, 2021
https://doi.org/10.37118/ijdr.21990.05.2021

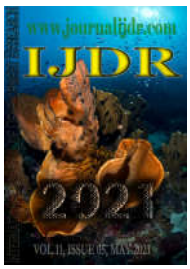

RESEARCH ARTICLE OPEN ACCESS

RESEARCH ON SIMULATION DESIGN OF WIRE ROPE DETECTION SENSOR BASED ON PERMANENT MAGNET EXCITATION

Binghua Chen and *Shangkun Ren

Key Laboratory of Non-destructive Testing Technology of Ministry of Education, School of Testing and Optoelectronic Engineering, Nanchang Hangkong University, Nanchang 330063, Jiangxi, China

ARTICLE INFO

Article History:
Received 20th February, 2021
Received in revised form
19th March, 2021
Accepted 16th April, 2021
Published online 30th May, 2021

Key Words:

Magnetic Flux Leakage Testing, Wire Rope Testing, Non-Destructive Testing, Permanent Magnet Excitation, Finite Element Simulation.

Corresponding author: Shangkun Ren

ABSTRACT

Permanent magnet excitation is the current mainstream excitation method for wire rope defect detection.Use Maxwell finite element simulation software to simulate the structure of the yoke in the permanent magnet excitation mode, and construct the optimal excitation structure through the analysis of the simulation data; The relationship between the placement height of the magnetic sensor and the change of the leakage magnetic field under the excitation structure is analyzed; The changes of leakage magnetic field under different defect lengths and different defect depths are studied; The change of the leakage magnetic field when the excitation structure is jittered is analyzed; And use matlab to fit some of these changes. The analysis of these data can play an important role in the development of detection probes for permanent magnet excitation.

Citation: ***Binghua Chen, Shangkun Ren,*** "Research on Simulation Design of Wire Rope Detection Sensor Based on Permanent Magnet Excitation", *International Journal of Development Research*, 11, (05), 47270-47275.

INTRODUCTION

With the current vigorous development of national infrastructure, steel wire ropes are recognized for their light weight, good elasticity, high tensile strength and fatigue resistance, and very stable working performance [Xiaolan *et al.,* 2017]. Wire rope is widely used in metallurgy, construction, mining, tourism, ports, transportation, petroleum exploration and military industry and other industries, its role is more and more obvious and the demand is also increasing [Fan Wei *et al.,* 2020]. Because the working environment of the wire rope is very bad, there are broken wires, abrasion, corrosion, etc., which makes the wire rope there is a huge hidden risk in the use process [Fan Wei *et al.,* 2020]. In recent years, the rupture of the wire rope has caused many accidents.For example, in 2017, a crane wire rope suddenly broke in Zhejiang, causing the steel pipe support to collapse, resulting in 1 death and 3 injuries;in 2019, the Yanzishan mine in Datong, Zhongshan, the Tongling construction site in Anhui, the Shimen iron mine in Linyi, Shandong, and the Donghu Scenic Area in Wuhan caused nearly 100 deaths due to defects such as broken wire ropes.There are more or less potential problems in the steel wire ropes currently in service, which requires the development of relevant instruments for testing. The current excitation methods mainly include DC excitation, AC excitation, permanent magnet excitation, and comprehensive excitation. These four excitation methods have their own advantages and disadvantages [Liu Liangliang, 2016], as shown in Table 1.By comparing the advantages and disadvantages of the four excitation methods listed in Table 1, it can be found that although permanent magnet excitation has the disadvantage of poor magnetization flexibility, it is more suitable for actual detection and use because of its light weight and convenient portability without power supply.Therefore, this simulation uses permanent magnet excitation for corresponding data simulation. Zhang Xin and others introduced the phenomenon of clutter in the current wire rope electromagnetic detection process, analyzed the specific reasons for the clutter in the detection process, and used Ansys finite element simulation software to analyze the changes of clutter at different lift-off heights [Zhang Xin, 2018]. Li Wanli and others used the method of combining the leakage flux method and the magnetic bridge circuit method to construct a new excitation structure, which can detect the defects of LF and LMA wire ropes at the same time,and by using the theoretical design and simulation verification of the excitation

structure to analyze and verify the excitation structure [Li Wanli, 2012]. Tian Jie and Zhao Caiyue use the principle of permanent magnet excitation to use the principle of magnetic flux leakage detection. By using the 3D module of Maxwell finite element simulation software,the relationship between the distance between the magnets at both ends of the wire rope, the lift-off value and the magnetic induction intensity is simulated,at the same time, the relationship between the Hall array and the magnetic induction intensity is discussed [Tian Jie, 2020].Wang Hongyao and others designed a mine wire rope defect detector system based on the principle of ultrasonic sight distance and strong magnetic detection. The strong magnetic detection device is used to detect wire rope breakage and wear,by using Maxwell to simulate and compare the excitation structure, it is concluded that the radial excitation method is more conducive to the detection of magnetic flux leakage signals by the magnetic sensor [Wang Hongyao, 2020].

The theoretical basis of model simulation of steel wire rope leakage magnetic field: The theoretical model of the magnetic dipole provides an important theoretical basis for the finite element simulation of the wire rope leakage magnetic field.The theoretical model of the magnetic dipole is shown in Figure 1.Use the related theory of magnetic field distribution to analyze and calculate the leakage magnetic field at the fracture.Assuming that the point P1 (-L, 0) and the point P2 (L, 0) at the fracture point have charges of +Q and -Q, respectively,According to the vector superposition theorem of the magnetic field, the magnetic induction intensity at the point P(x,y) is equal to the vector sum of the magnetic field intensity generated by the two points P1 and P2 at the point P,The components of the magnetic field strength at point P in the x and y directions are [Shi Rong, 2014]:

$$B_{px} = B_{1x} + B_{2x} = \frac{Q}{4\pi}\{\frac{x-\delta}{[(x-\delta)^2+y^2]^{\frac{3}{2}}} - \frac{x+\delta}{[(x+\delta)^2+y^2]^{\frac{3}{2}}}\} \quad (1)$$

$$\Delta B_{py} = B_{1y} + B_{2y} = \frac{Q}{4\pi}\{\frac{y}{[(x-\delta)^2+y^2]^{\frac{3}{2}}} - \frac{y}{[(x+\delta)^2+y^2]^{\frac{3}{2}}}\} \quad (2)$$

In the formula, x represents the axial direction along the wire rope, and y represents the radial direction along the wire rope.

Set the diameter of the wire rope as D, then the length of the fracture is $2\delta - D$, The magneticcharge Q at the fracture is:

$$Q = \frac{\pi B_g D^2}{4} \quad (3)$$

Where B_g is the magnetic induction intensity (T) in the wire rope.

Simulation analysis of the influence of changes in related parameters on the distribution of leakage magnetic field: Use the 2D module of Maxwell2019R3 finite element simulation software to carry out the data simulation of the corresponding size structure and defects. The excitation structure model is shown in Fig. 2.A in Fig.2 represents a steel wire rope with a length of 240mm and a diameter of 8mm;B represents a detection line with a length of 10mm and a distance of 3mm from the surface of the wire rope;C represents a rectangular defect with a length of 2mm and a depth of 2mm;D stands for permanent magnet, the material uses N35 neodymium iron boron;E means armature, the material used is industrial pure iron;F indicates that the distance between two neodymium iron boron is the inner length of the yoke;G indicates that the length of NdFeB is the inner width of the yoke; H indicates the width of NdFeB; I indicates the width of the armature.

The relationship between the leakage field and the size change of the excitation structure: The related simulation of the excitation structure mainly includes the following four parts: the relationship between the change of the inner length F, the inner width G, the NdFeB width H, the armature width I and the magnetic flux density of the leakage field.And based on the simulation of the above four parts, the optimal yoke excitation structure is obtained, and on the basis of this yoke excitation structure, the four types of defect length, defect depth, detection line lift-off, and yoke lift-off fluctuation are carried out. The simulation of the aspect, the corresponding change relationship is obtained. First, simulate the relationship between the change of the NdFeB width H and the change of the magnetic flux density of the leakage field.Here, the specific data of the yoke is first set as: inner length F=80mm, inner width G=20mm, armature width I=20mm,the change range of the NdFeB width H is set at 10mm-60mm, increasing by 10mm in turn.The results of the obtained axial component and the radial component show that the curve changes with the width of NdFeB to be the same.Therefore, only the relevant results of the Bx axial component are attached as shown in Fig.3. From the two figures in Fig.3, it can be seen that the leakage magnetic field changes rapidly when the width of NdFeB is between 10mm-30mm, and the change of the leakage magnetic field is gentle to stable between 30mm-60mm.And when the NdFeB width H=30mm, the leakage field strength reaches 70mT, so when the diameter of the wire rope is 8mm, the NdFeB width of 30mm can meet the requirement. According to the simulation data of NdFeB, the relationship of the leakage magnetic field with the internal width G is carried out.Here, the NdFeB width H=30mm, the inner length F and the armature width I remain unchanged, and the change range of the inner width G is set to 20mm-60mm, increasing by 10mm in turn.By sorting out the results of the axial component and radial component, it is found that the change trends of the two are the same.Only the axial component leakage magnetic field change diagram with different inner width width and the curve change diagram above the defect under different inner width width are attached here as shown in Fig.4: It can be seen from the two graphs in Fig.4 that as the inner width increases, the leakage magnetic field changes show a tendency to increase first and then stabilize.From Fig.4b, it can be concluded that when the inner width reaches 50mm, the leakage magnetic field changes have tended to the peak, that is, when the inner width G=50mm, the leakage magnetic field reaches the maximum. According to the above two simulation data, the relationship between the change of armature width and the change of leakage magnetic field is studied.Here, the inner length F remains unchanged, the inner width G=50mm, and the NdFeB width H=30mm.Set the change range of the armature between 5mm-25mm, increasing by 5mm in turn.After sorting out the axial component data and the radial component data, it is found that the changing trends of the two are similar.

Only the axial component leakage magnetic field with different armature widths and the change of the upper defect curve under different armature widths are shown in Fig.5Show: It can be seen from the two figures in Fig.5 that as the armature width increases, although the leakage magnetic field increases faster between 5mm-20mm, it reaches the peak at 20mm and no longer increases and shows a decreasing trend. That is, when the armature width I=20mm, the leakage magnetic field can reach the peak point. According to the above simulation data of the NdFeB width, inner width, and armature width, the relationship between the change of the inner length and the change of the leakage magnetic field is simulated.Here, based on the above results, set the NdFeB width H=30mm, the inner width G=50mm, and the armature width I=20mm.The change range of the inner length is set between 40mm-160mm, increasing by 30mm in turn.After sorting out the data, it is found that the change trajectory of the axial component and the radial component are similar.Only the axial component leakage magnetic field change diagram with different inner length lengths and the curve change diagram above the defect under different inner length lengths are attached here as shown in Fig.6. According to the two figures in Fig. 6, it can be seen that as the inner length increases, the overall change of the leakage magnetic field shows a decreasing trend.It can be seen from Fig. 6b that when the range is between 40mm-160mm, the variation range of the leakage magnetic field at this time is between 65mT-75mT.By using matlab fitting to fit the change trend of the internal length and the axial component leakage magnetic field into a formula, the

Table 1. Advantages and disadvantages of different excitation methods

Excitation method	Advantage	Disadvantage
AC excitation	Low cost, simple structure, flexible control of magnetization	There is eddy current loss, skin effect, low penetration depth of detection
DC excitation	The detection depth is large, and the magnetization intensity can be flexibly controlled	Need to be equipped with a stable, large DC power supply, and a large excitation device
Permanent magnet excitation	Light weight, small size, no power supply, easy maintenance	Can not adjust the magnetization flexibly, and the flexibility of magnetization is poor
Comprehensive excitation	Reduce the influence of material uniformity and permeability changes, and the detection effect is better	The signal processing is relatively complicated, and the excitation device design is relatively complicated

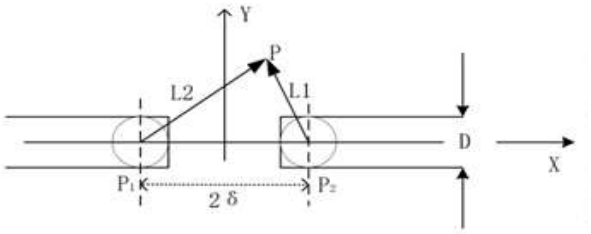

Fig.1 Magnetic dipole model

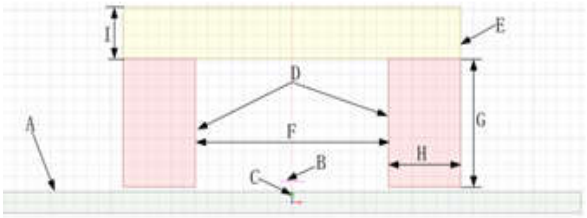

Fig. 2 Excitation structure model

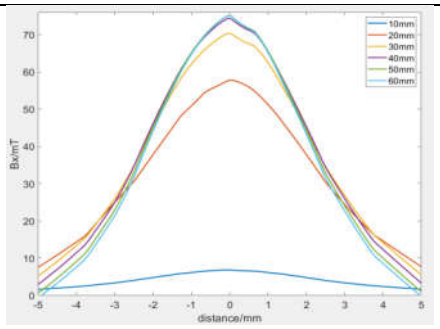

Fig. 3a. The distribution diagram of the axial component leakage magnetic field with the width of NdFeB

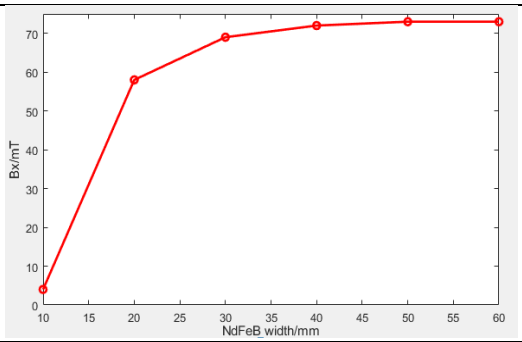

Fig. 3b. The curve change of the defect above the defect under different NdFeB width

Fig. 3. The relationship between the width of NdFeB and the axial component and the leakage magnetic field above the defect

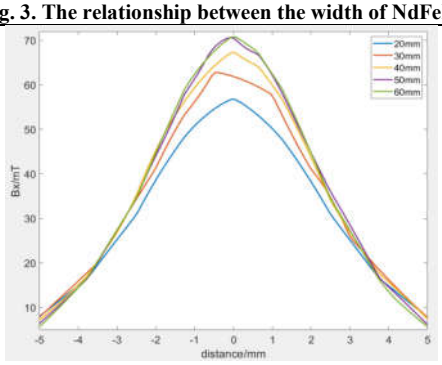

Fig.4a. The axial component leakage magnetic field changes with different inner widths

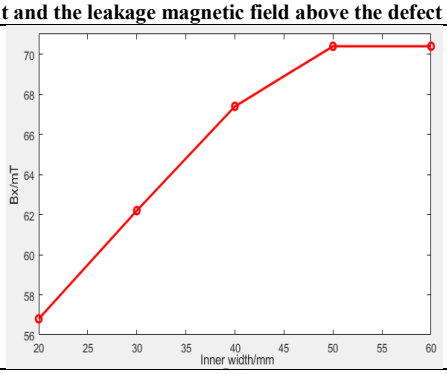

Fig. 4b. The change of the curve above the defect under different internal widths

Fig. 4. The axial component and the leakage magnetic field above the defect change with different internal widths

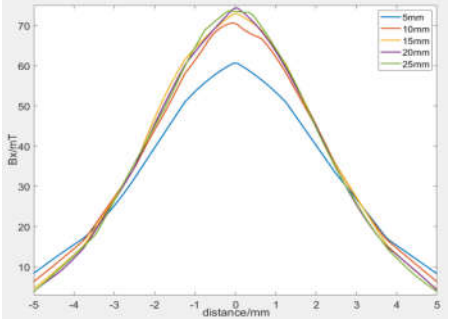

Fig. 5a. The axial component leakage magnetic field changes with different armature widths

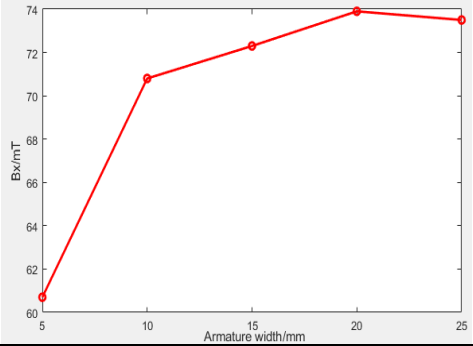

Fig. 5b. The curve change diagram above the defect under different armature width

Fig. 5. The relationship between the axial component and the leakage magnetic field above the defect with the width of the armature

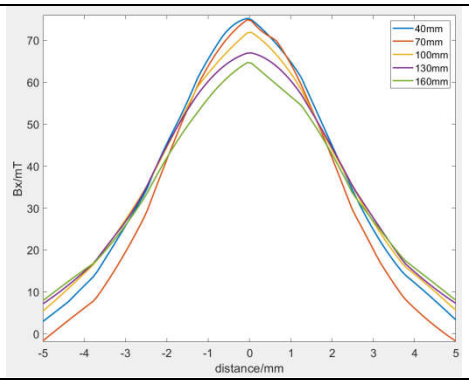

Fig. 6a. The axial component leakage magnetic field changes with different inner lengths

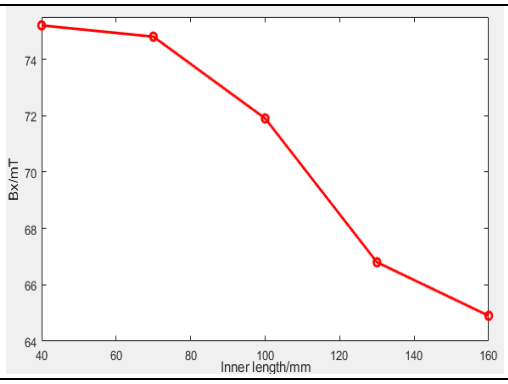

Fig. 6b. The curve change diagram above the defect under different inner lengths

Fig. 6. The relationship between the axial component and the leakage magnetic field above the defect with the change of the inner length

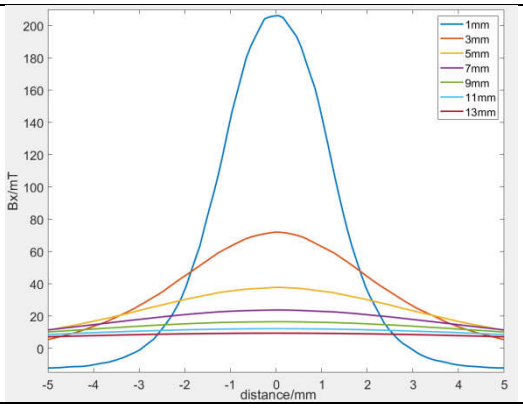

Fig. 7a. The axial component leakage magnetic field changes with different lift-off heights

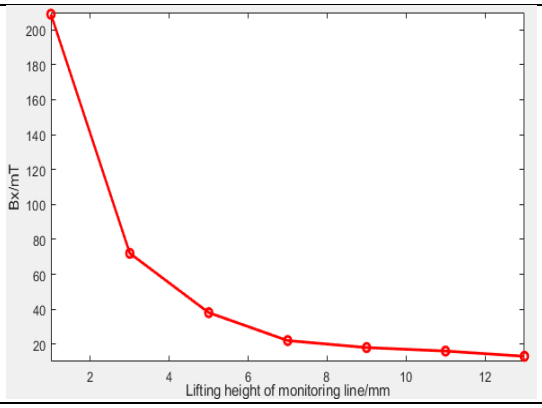

Fig. 7b. The curve change diagram above the defect under different lift-off heights

Fig. 7. The axial component and the leakage magnetic field above the defect change with the lift-off height

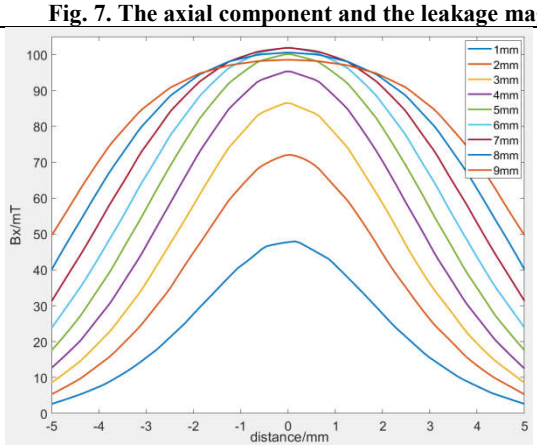

Fig. 8a. The axial component leakage magnetic field changes with different defect lengths

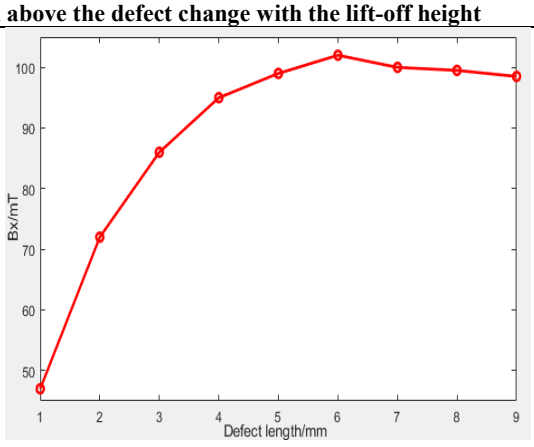

Fig. 8b. The curve change diagram of the upper axial component defect under different defect lengths

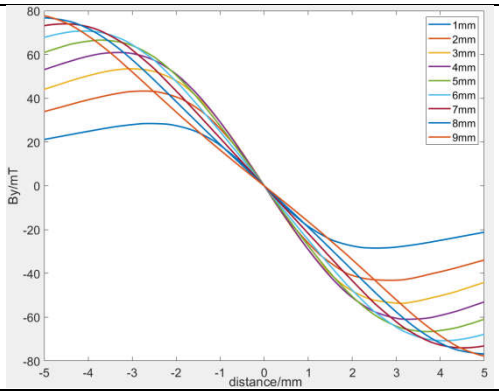

Fig. 8c. The radial component leakage magnetic field changes with different defect lengths

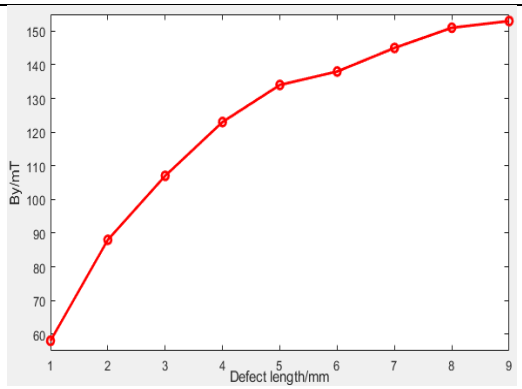

Fig. 8d. The change of the curve above the radial component defect under different defect lengths

Fig. 8. Axial and radial relationship diagram of leakage magnetic field with defect length

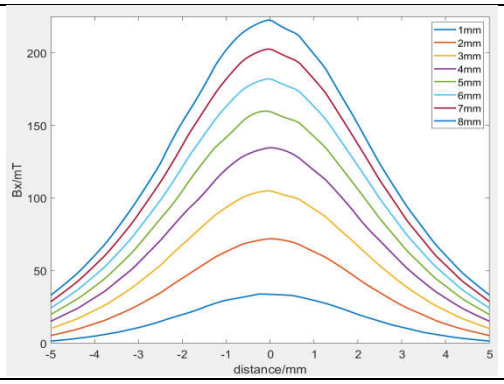

Fig. 9a. The axial component leakage magnetic field changes with different defect depths

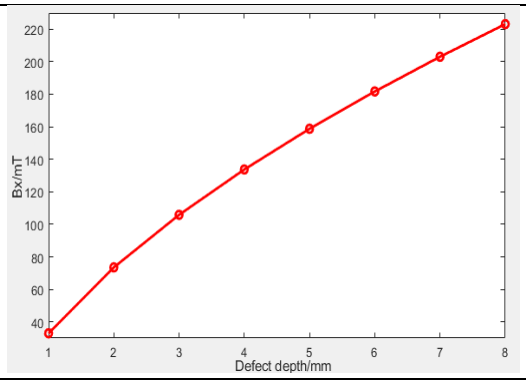

Fig. 9b. The change of the axial component defect at different depths

Fig. 9. The axial component and the leakage magnetic field above the defect change with the depth of the defect

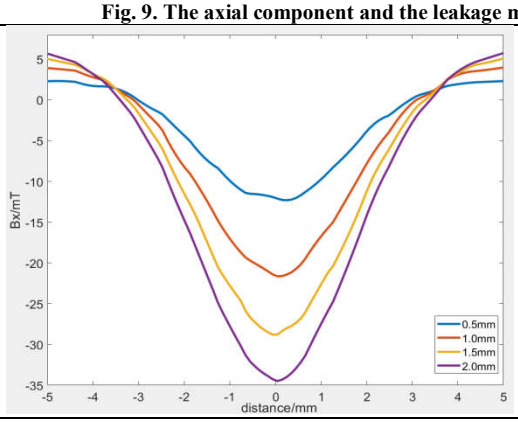

Fig.10a. The curve change diagram under different fluctuation heights at a relatively unfluctuation position

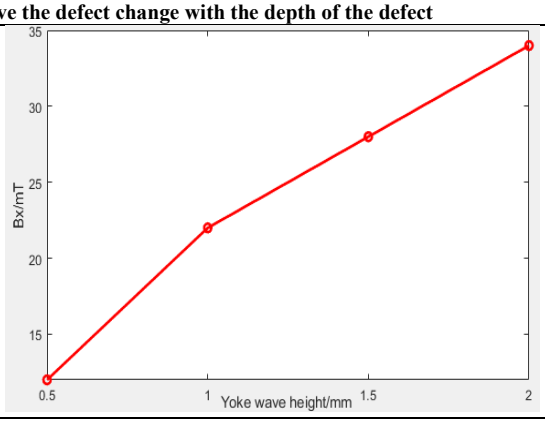

Fig. 10b. The curve change of the numerical value reduction curve above the defect under different fluctuation heights relative to the unfluctuation position

Fig. 10. The fluctuation graph and the graph of the value above the defect with the fluctuation height curve

approximate formula isB_x=-0.001233$f^{1.82}$+76.8.The specific inner length selection can be determined according to the specific upper and lower limits of the selected magnetic sensor. Here, the inner length F is set to 100mm for the subsequent defect detection simulation. According to the above four sets of simulations for the yoke size data, through the analysis of the data, it can be concluded that when the diameter of the wire rope is 8mm,NdFeB width H=30mm, armature width I=20mm, inner width G=50mm (that is, the length of NdFeB 50mm), and inner length F=100mm (that is, the distance between the two permanent magnets is 100mm, and the total length of the armature is 160mm). The excitation intensity of the magnetic yoke can make the magnetic sensor more sensitive to defect detection.

The relationship between the leakage magnetic field and the height of the sensor: In the process of developing the detection probe, the placement height of the magnetic sensor is a problem that needs to be paid attention to.For the wire rope detection process, the monitoring probe is closely attached to the surface of the wire rope for movement detection, that is, there is a certain range for the placement height of the magnetic sensor.If it is placed low, although the detection sensitivity will be improved to a certain extent, the thickness of the outer protective material of the yoke will be very thin, which will shorten the service life of the protective material;If it is placed too high, the detection sensitivity will be reduced, so the magnetic sensor should be placed at a certain appropriate height. Here, the placement height range of the detection line (representing the magnetic sensor) B is set between 1mm-13mm on the surface of the wire rope, increasing by 2mm in turn.The analysis of the data of the axial component and the radial component shows that the curves of the two are similar.Here only the variation of the axial component leakage magnetic field with different lift-off heights of the detection line and the variation of the curve above the defect at different heights are shown in Fig.7. Through the analysis of the two graphs in Fig. 7, as the detection straight line lift-off height increases, the leakage magnetic field will decrease, and the decrease is very large between 1mm-7mm.When it is between 7mm-13mm, the decreasing amplitude is smaller and tends to be stable. By using the data fitting of matlab, the relationship between the axial component leakage magnetic field and the detection straight line lift-off height h can be fitted toB_x=330.$5^{-0.8139h}$+69.$79^{-0.1588h}$.Therefore, when considering the placement height of the magnetic sensor, a height of 1mm-7mm is appropriate. Considering the thickness of the outer protective material of the yoke, the placement height of the magnetic sensor can be placed in the range of 3mm-7mm.Here, the height of the detection line is set at 3mm.

The relationship between the leakage magnetic field and the defect length: According to the previous simulation of relevant data, the relationship between the length of the wire rope defect and the change of the leakage magnetic field was simulated.Here, the depth of the defect is set to 2mm, and the range of the length of the defect is set to be between 1mm-9mm, increasing by 1mm in turn.After sorting and analyzing the data obtained from the simulation, it is found that the relationship between the axial component and the radial component is quite different.Attached here are the changes in the axial component leakage magnetic field with different defect lengths and the changes in the curve above the defect under different defect lengths,the variation of the radial component leakage magnetic field with different defect lengths and the variation of the difference between peaks and troughs under different defect lengths are shown in Fig. 8. It can be seen from Fig.8a and Fig. 8b that as the length of the defect increases in the axial component, the leakage field will first increase to a peak and then begin to decrease.It can be seen from Fig.8b that the leakage magnetic field changes faster when the defect length is between 1mm-6mm, and the leakage magnetic field begins to decrease when the defect length is between 6mm-9mm.Within these two ranges, the slope of the former segment is greater than the slope of the latter segment, and reaches a maximum when the defect length is 6mm.From the axial component, it can be seen that there is a double value situation, that is, two results appear under the same magnetic field strength,in this case, it is difficult to judge the specific

defect length based on the obtained waveform diagram;In Fig. 8c and Fig. 8d, it can be seen that as the length of the defect increases, the leakage magnetic field will increase, and there will be no double value.By comprehensively considering the two components of the axial component and the radial component, the specific length of the wire rope defect can be judged more accurately.Through the use of matlab fitting, we can get: the change trajectory of the axial component curve is fitted into $B_x=145.6^{-0.03856l}-135.3^{-0.3817l}$;The change trajectory of the radial component curve can be fitted into $\Delta B_y=-1445l^{-0.03353}+1500$.

The relationship between the leakage magnetic field and the depth of the defect: Here, the length of the defect is set at 2mm, and the range of defect depth is set at 1mm-8mm, increasing by 1mm in turn.Analyzing and sorting out the obtained simulation data, it is found that the change trajectories of the axial component and the radial component are similar.Attached here is the variation diagram of the axial component leakage magnetic field with different defect depths and the variation diagram of the curve above the defect under different defect depths, as shown in Fig. 9. It can be seen from the two figures in Fig. 9 that as the depth of the defect increases, the leakage magnetic field will increase.By using matlab to fit the change trajectory above the axial component defect under different defect depths as$B_x=83.66d^{0.5703}-50.72$.

The influence of the yoke lift-off fluctuation on the leakage magnetic field: In the process of testing the steel wire rope, the detection probe is closely attached to the surface of the steel wire rope, which can improve the sensitivity of detection.The service environment of the wire rope is relatively harsh. If the surface of the wire rope is rusted, raised or shaken during the detection process, the detection sensitivity of the wire rope will be affected.Here, the length and depth of the defect are both set to 2mm, and the detection jitter range is set to be between 0mm-2mm, with an increase of 0.5mm in turn.The relatively non-fluctuating place is the change of the difference of each wave height at 0mm and the change of the difference of the defect above the defect under different wave heights are shown in Fig.10:

CONCLUSION

- Through the simulation of the four parts of the yoke excitation structure: NdFeB width, inner width, armature width, and inner length.It is better to have a structure with NdFeB width H=30mm, inner width G=50mm, and armature width I=20mm.For the inner length, the larger the inner length, the smaller the leakage magnetic field. Therefore, the specific length setting for the inner length can be specifically determined according to the upper and lower limits of the magnetic sensor.
- The placement height range of the magnetic sensor should be set between 3mm-7mm on the surface of the wire rope.
- In the relationship between the length of the defect and the leakage magnetic field, there is a double value in the axial component. When judging the specific length of the defect, the waveform changes of both the axial component and the radial component should be considered comprehensively.
- The deeper the defect depth, the greater the value of the leakage magnetic field.
- The greater the lift-off fluctuation height of the yoke, the greater the reduction in the value of the leakage magnetic field detected at the place where the yoke is not fluctuated. This requires that the wire rope detection process should be as stable as possible.

Acknowledgement: Project supported by the National Natural Science Foundation of China (51865039）

REFERENCES

Fan Wei, Li Bing, Chen Binghua, et al. 2020. Analysis of electromagnetic non-destructive testing techniques for stress concentration and fatigue damage of steel wire ropes[J]. Electromechanical Information, (12): 144-147+149.

Fan Wei, Li Bing, Chen Binghua, et al. 2020. Research on the evaluation method of electromagnetic non-destructive testing ability for wire rope damage[J]. China Equipment Engineering, (13): 152-154.

Li Wanli, Feng Wenjie, Li Zhenzhen, et al., 2012. Design of excitation structure size for wire rope defect detection[J]. Journal of Tongji University (Natural Science Edition), 40(12):1888-1893.

Liu Liangliang. 2016. Research on steel wire rope fatigue damage detection based on magnetic characteristic parameters [D]. Qingdao Technological University.

Shi Rong,Guo Peng,Wang Jindong, et al. 2014. Research on wire rope flaw detection technology based on weak magnetic field [J]. Acta Metrology Institute, 35(1):78-82.

Tian Jie, Zhao Caiyue. 2020. Simulation research on wire rope magnetic flux leakage detection based on 3D Maxwell[J]. Coal Engineering, 52(07): 152-156.

Wang Hongyao, Li Xiaowei, Han Yimiao, et al. 2020. Design of mine wire rope damage detection system [J]. Industry and Mine Automation, 46(6): 92-97

Xiaolan Yan,Donglai Zhang, Fei Zhao. 2017. Improve the signal to noise ratio and installation convenience of the inductive coil for wire rope nondestructive testing[J].NDT&E International, 92(12): 221-227

Zhang Xin, Xia Huaming, Zhang Chenxu, et al. 2018. Research on clutter of electromagnetic detection signal of mine hoist wire rope[J]. Coal Engineering, 50(8):119-121.

****